

Modulating Heme Redox Potential Through Protein-Induced Porphyrin Distortion

Charles Olea, Jr.,[†] John Kuriyan,[†] and Michael A. Marletta^{*†}

*Departments of Molecular and Cell Biology and Chemistry, California Institute for
Quantitative Biosciences, Howard Hughes Medical Institute, and Division of Physical
Biosciences, University of California, Berkeley, Berkeley, CA 94720-3220*

*marletta@berkeley.edu

Index	Page
Figure S1	2
Figure S2	3
Figure S3	4
Experimental details	5
Structural alignment and resonance Raman discussion	9
Table S1	10
Table S2	11
Table S3	12
References	13

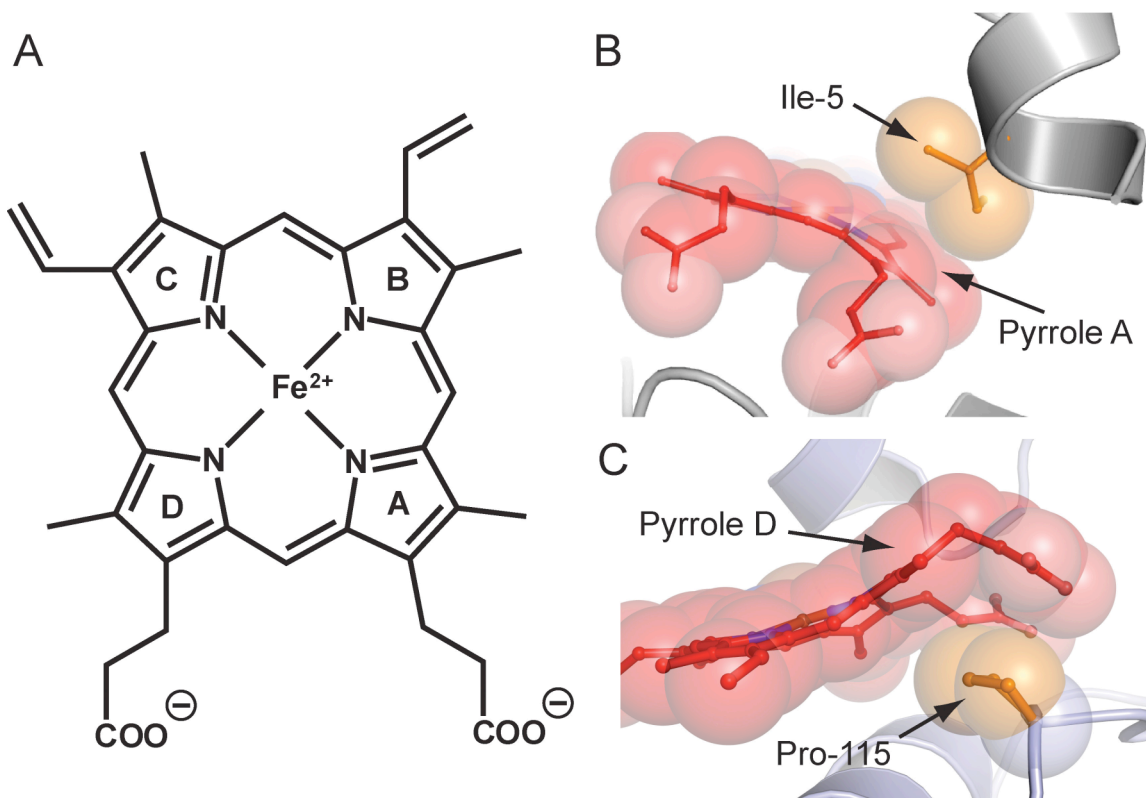


Figure S1. Heme Distortion in wild-type *Tt* H-NOX. A) Heme prosthetic group with pyrrole groups A-D labeled. B) Ball-and-stick and space filling model of Ile-5 and C) Pro-115 and the surrounding heme environment of wild-type *Tt* H-NOX. Ile-5 and Pro-115 push down and up against the heme, respectively, causing pronounced kinks in the heme. Out-of-plane distortions up to 2 Å are observed in the crystal structure. The I5L mutation caused a disruption of the pyrrole A and γ/δ carbon interaction, which allowed the heme cofactor to relax and become planar. The P115A mutation eliminates the steric bulk at the proximal side of the heme and allows pyrrole D to move into the plane. The effect of the double mutation I5L/P115A was not additive. The two mutations appeared to counterbalance each other and the degree of heme distortion was higher than the single mutant P115A. Since, the I5L/P115A double mutant displayed a distinct degree of distortion it was included in subsequent analyses.

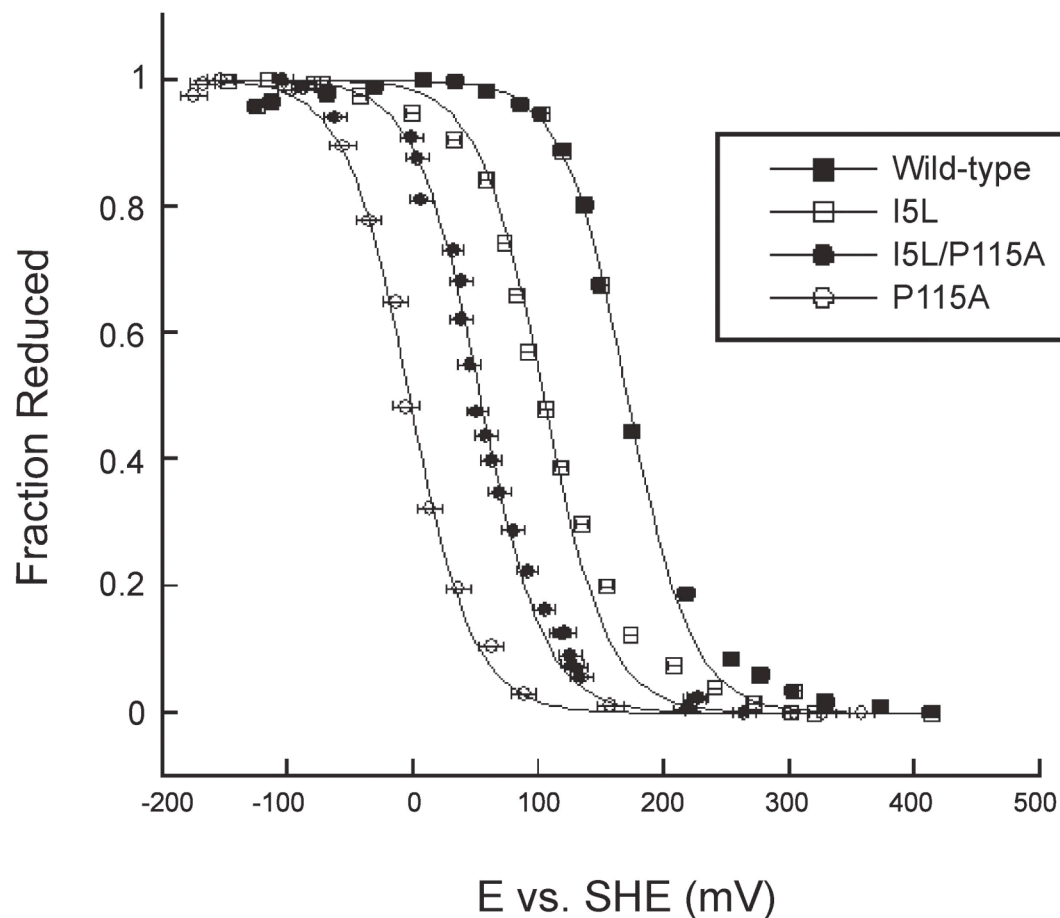


Figure S2. Reduction Potential of wild-type and mutants. The reduction potential was measured and calculated as described.^{5,8} Titration curves for wild-type¹, I5L, I5L/P115A, and P115A¹ were determined against the standard hydrogen electrode (SHE). The ratio of reduced Fe²⁺ to oxidized Fe³⁺ heme was measured based on their α/β maximum at approximately 557 (reduced) nm for wild-type and I5L. The difference absorbance of the α/β maximum for reduced and the α/β minimum for oxidized was used to calculate the fraction reduced for I5L/P115A and P115A. The voltage against the SHE was measured for both oxidative and reductive titrations of the wild-type protein and the mutants. Error bars represent the standard error for wild-type and P115A and range and standard deviation for I5L and I5L/P115A, respectively.

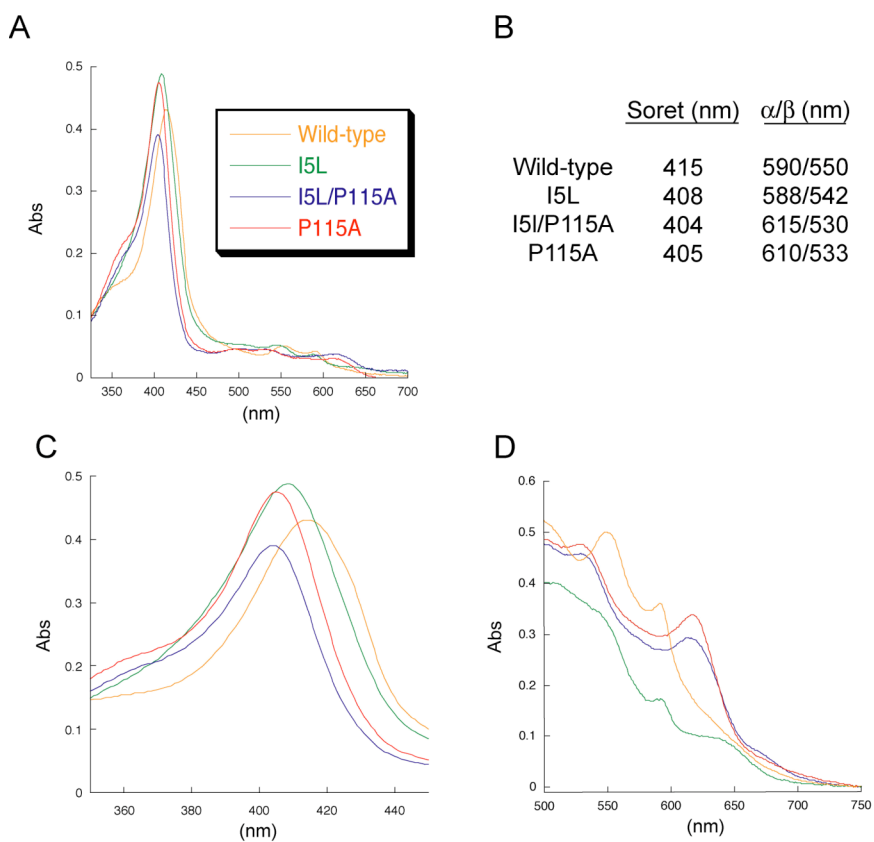


Figure S3. Ferric Spectra of the Tt H-NOX wild-type protein and mutants. A) Full spectra of wild-type and mutants. B) Values for λ max of the Soret and α/β regions. Panel C) shows a more detailed Soret region and D) α/β regions of wild-type protein and mutants.

Experimental details

Expression of the I5L and I5L/P115A mutants of *Tt* H-NOX in *E. coli*. Mutagenesis, cell culture, and expression procedures were carried out as previously described.²

Purification of the I5L and I5L/P115A mutants in *E. coli* for crystallization and potentiometry. Cell lysis and thermal treatment were carried out as described with the exception of an ultracentrifugation step after cell lysis.² After thermal treatment the supernatant was loaded onto a Toyopearl Q 650M anion exchange column that was equilibrated buffer A (50 mM TEA, pH 7.5, and 50 mM NaCl) at a flow rate of 1.5 mL/min. The flow-through was passed down a Sephadex G-25 column equilibrated in buffer B (50 mM HEPES pH 6.25). The red-colored flow through was collected and loaded on a SP 650M cation exchange column equilibrated in buffer B at 1 mL/min. The protein was eluted off the cation exchange column with a salt gradient of 0-40% buffer C (50 mM HEPES and 500 mM NaCl pH 6.25) at 1 mL/min in 2 mL fractions were collected. Red-colored fractions were initially pooled based on Coomassie stain and for subsequent runs based on a Soret: A_{280} ratio above 1.6. Both I5L and I5L/P115A were isolated as the Fe(II)-O₂ complex², and stored at -80 °C in a final buffer of 50 mM HEPES, 200 mM NaCl, and 5% glycerol at pH 6.25.

Crystallization of the I5L mutant. Samples of I5L were equilibrated with 20 mM TEA pH 7.5 and concentrated to 25 mg/mL. Orthorhombic crystals were grown by sitting drop vapor diffusion by mixing 1 μ L of protein solution with 4 μ L of the reservoir solution and equilibrating against 700 μ L of 0.1 M MES pH 6, 0.1 M LiCl, and 26%

polyethylene glycol 4000 for two days at 16 °C. Cryoprotection was achieved by addition of mother liquor substituted with 30% glycerol in increasing glycerol amounts of 5% to a final concentration of 15% glycerol, flash frozen, and stored in liquid nitrogen.

Crystallization of the I5L/P115A mutant. Samples of I5L/P115A were equilibrated with 20 mM TEA pH 7.5 and concentrated to 30 mg/mL. Monoclinic crystals were grown by sitting drop vapor diffusion by mixing 1 μ L of protein solution with 3 μ L of the reservoir solution and equilibrating against 700 μ L of 0.05 M MES pH 6, 0.1 M LiCl, and 22% polyethylene glycol 4000 for two days at 16 °C. Cryoprotection was achieved by addition of mother liquor substituted with 40% glycerol in increasing amounts of 5% glycerol to a final concentration of 25% glycerol, flash frozen, and stored in liquid nitrogen.

X-ray data collection, phasing, and refinement of the I5L mutant. X-ray data were collected by using synchrotron radiation at beamline 8.2.1 at the Advanced Light Source, Lawrence Berkeley National Laboratory. Diffraction images were collected at 100 K with 7 s exposure time and 1° oscillations per frame. Data were processed with the HKL2000 suite.³ Molecular replacement was carried out with the CCP4 program Phaser⁴ using P115A H-NOX (PDB ID: 3EEE) as the search model. Model building was carried out by using the program Coot⁵ and refinement was carried out using CNS and Phenix with TLS refinement parameters incorporated. The final model includes 2 I5L molecules in the asymmetric unit. The structure of I5L was refined to a final overall R_{work} and R_{free} of 21.7% and 26.0% at 2.15 Å resolution, respectively.

X-ray data collection, phasing, and refinement the I5L/P115A mutant. X-ray data were collected by using synchrotron radiation at beamline 8.2.1 at the Advanced Light Source, Lawrence Berkeley National Laboratory. Diffraction images were collected at 100 K with 5 s exposure time and 1° oscillations per frame. Data processing, phasing, model building and refinement were carried out as described above. The final model includes 2 I5L/P115A molecules in the asymmetric unit. The structure of I5L/P115A was refined to a final overall R_{work} and R_{free} of 18.9% and 23.5% at 2.04 Å resolution, respectively.

Spectrophotometric Redox Titrations of the I5L and I5L/P115A mutants.

Potentiometric titrations of I5L and I5L/P115A were performed as described previously.^{1,6} Plotted is the mean rms deviation from planarity of wild-type and mutants versus the mean reduction potential against SHE. The error bars for the potential represent the standard error for wild-type and P115A and the range and standard deviation for I5L and I5L/P115A. The vertical bars for the rmsd from planarity represent the range of values for all molecules in the AU for each protein.

pH titration of wild-type and mutants. Protein (5.6 μM) was equilibrated in 50 mM titrant buffer and 50 mM NaCl at 25 °C. The protein sample was titrated with 50 mM buffer from pH 5.00-9.61 (acetate pH 5.00; MES pH 5.43, 6.03, and 6.50; HEPES pH 7.07, 7.52, and 7.96; and Bis-TRIS propane 8.53, 9.03 and 9.61). The protonation state of the distal water was measured by the difference of absorbance at the Soret maximum.

Titration curves for wild-type and I5L were fit to the Henderson-Hasselbalch equation. Error bars for wild-type and I5L represent the standard deviation. The pK_a values for I5L/P115A and P115A could not be determined within the range of the experiment due to protein instability.

All structures were overlaid and compared with monoclinic wild-type molecule A since it has the highest degree of heme distortion. It is important to note that the crystallographic data are in agreement with solution resonance Raman data.⁸ All analyses probing the chemical properties were carried out in solution; therefore it is important that solution experiments are congruent with the crystallographic data.

Table S1. Statistics of crystallographic data collection and refinement statistics		
	I5L	I5L/P115A
<i>Data Collection</i>		
Space group	<i>P</i> 2 ₁ 2 ₁ 2	<i>C</i> 2
Cell dimensions		
<i>a</i> , <i>b</i> , <i>c</i> (Å)	79.825, 126.095, 42.742	127.158, 79.828, 43.322
α , β , γ (°)	90	$\beta = 102.25$
Resolution (Å)	2.15	2.04
R_{merge} (%)	6 (42)	5 (14)
I / σ^a	24.7 (4.8)	22.7 (8.3)
Completeness ^a (%)	99.5 (99.8)	99.4 (95.0)
Redundancy	6.7	3.7
<i>Refinement</i>		
No. of reflections	23163	25754
$R_{\text{work}} / R_{\text{free}}^b$ (%)	21.7/26.0	18.9/23.4
No. atoms		
Protein	2935	3098
Heme	86	86
O ₂ Molecules	2	2
Solvent molecules	55	145
Overall <i>B</i> -factors	43.8	26.0
Rmsd Bond lengths (Å)	0.010	0.009
Rmsd Bond angles (°)	1.035	1.060
^a The values in parentheses relate to highest-resolution shells.		
^b R_{free} is calculated for a randomly chosen 5% of reflections.		

Table S2. Heme deviations from planarity of mutants of and wild-type *Tt* H-NOX^a

	rms deviation ^b	Saddling ^c	Ruffling ^c	Tilt ^f (degrees)
I5L				
Heme A	0.34	-0.832	-0.634	81
Heme B	0.34	-0.816	-0.758	79
I5L/P115A				
Heme A	0.20	-0.448	-0.216	88
Heme B	0.16	-0.415	-0.261	86
P115A ^d				
Heme A	0.22	-0.499	-0.612	80
Heme B	0.22	-0.395	-0.766	84
Heme C	0.12	-0.043	-0.488	88
Heme D	0.15	0.066	-0.517	87
Wild-type monoclinic ^e				
Heme A	0.46	-1.069	-1.105	78
Heme B	0.33	-0.634	-0.814	86
Wild-type orthorhombic ^e				
Heme A	0.45	-1.092	-1.094	80
Heme B	0.44	-0.994	-1.210	81

^aFe(II)-O₂ complexes.

^brms deviation from planarity in angstroms.

^cHeme conformations calculated using normal-coordinate analysis^{9,10}. The numerical value shown is the displacement along the normal mode in Angstroms.

^d1

^e10

^fCalculated using the least squares plane of the 4 pyrrole nitrogens in the heme (other atoms were excluded due to the high degree of distortion) and the five imidazole ring atoms of H102 in MOLEMAN2⁷. The acute angle is shown.

Table S3. Heme deviations from planarity in the crystal structure of P115A

Angles between pyrrole groups in P115A and wild-type H-NOX ^a						
	Φ A-B	Φ B-C	Φ C-D	Φ D-A	Φ A-C	Φ B-D
I5L						
Heme A	10.58	6.97	26.14	21.01	17.08	24.69
Heme B	11.02	12.42	23.84	19.18	21.05	23.90
I5L/P115A						
Heme A	2.21	6.46	18.13	14.72	8.10	13.92
Heme B	1.29	8.19	13.74	9.53	8.20	10.81
P115A ^b						
Heme A	8.86	12.04	14.26	10.25	15.22	16.35
Heme B	8.65	12.71	17.05	11.15	16.55	17.43
Heme C	1.16	10.43	8.79	8.35	9.71	9.51
Heme D	10.31	15.20	9.88	0.28	9.69	10.07
Wild-type orthorhombic ^c						
heme A	15.30	20.00	29.30	23.00	32.10	28.00
heme B	21.80	15.20	28.00	23.90	30.90	31.80
Wild-type monoclinic ^c						
heme A	17.30	18.20	24.10	27.30	32.60	27.40
heme B	15.90	9.80	26.90	11.50	16.50	27.40

^a Φ A-B, Φ B-C, etc. refer to the angles in degrees between the planes formed by pyrrole groups A and B, and B and C, respectively.

^b 1

^c 10

References

- (1) Olea, C., Jr.; Boon, E. M.; Pellicena, P.; Kuriyan, J.; Marletta, M. A. *ACS Chem. Biol.* **2008**, *3*, 703-710.
- (2) Karow, D. S.; Pan, D.; Tran, R.; Pellicena, P.; Presley, A.; Mathies, R. A.; Marletta, M. A. *Biochemistry* **2004**, *43*, 10203-10211.
- (3) Otwinowski, Z.; Minor, W. *Macromol. Cryst., Part A* **1997**, *276*, 307-326.
- (4) McCoy, A. J.; Grosse-Kunstleve, R. W.; Storoni, L. C.; Read, R. J. *Acta Crystallogr., Sect. D* **2005**, *61*, 458-464.
- (5) Emsley, P.; Cowtan, K. *Acta Crystallogr., Sect. D* **2004**, *60*, 2126-2132.
- (6) Dutton, P. L. *Methods Enzymol.* **1978**, *54*, 411-435.
- (7) Kleywegt, G. J.; Jones, T. A. *Acta Crystallogr., Sect. D* **1999**, *55*, 941-944.
- (8) Tran, R.; Boon, E. M.; Marletta, M. A.; Mathies, R. A. *Biochemistry* **2009**, *48*, 8568-8577.
- (9) Jentzen, W.; Ma, J. G.; Shelnuitt, J. A. *Biophys. J.* **1998**, *74*, 753-763.
- (10) Pellicena, P.; Karow, D. S.; Boon, E. M.; Marletta, M. A.; Kuriyan, J. *Proc. Natl. Acad. Sci. U.S.A.* **2004**, *101*, 12854-12859.